Pathology – Research and Practice 212 (2016) 1027–1033

Contents lists available at ScienceDirect

Pathology – Research and Practice

journal homepage: www.elsevier.com/locate/prp

Original article

Effects of an early intervention using human amniotic epithelial cells in a COPD rat model

Limei Geng[a,b], Zhiqiang Chen[a,c,*], Hong Ren[d], Xiaoyan Niu[a], Xiangyan Yu[b], Hongqian Yan[b]

[a] Graduate School, Hebei Medical University, Shijiazhuang 050017, China
[b] Department of Respiratory Medicine, the Traditional Chinese Medical Hospital of Hebei Province, Shijiazhuang 050011, China
[c] Department of Internal Medicine, the Traditional Chinese Medical Hospital of Hebei Province, Shijiazhuang 050011, China
[d] Department of Internal Medicine, Halixun Hospital, Hengshui 053000, China

ARTICLE INFO

Article history:
Received 21 September 2015
Received in revised form 7 July 2016
Accepted 30 August 2016

Keywords:
COPD rat model
Human amniotic endothelial cells
Early intervention
Interleukin-8
Matrix metalloproteinase 2
Matrix metalloproteinase 8

ABSTRACT

The study aimed to investigate the effect of an early intervention using human amniotic epithelial cell (hAEC) in a rat model of chronic obstructive pulmonary disease (COPD). Twenty-four specific pathogen-free Wistar rats were randomized to the control, COPD, and COPD + hAEC groups. COPD was established by intratracheal LPS injection combined with smoke fumigation over 30 days. On the first day of model establishment rats in the AEC group also received intratracheal instillation of 500,000 hAECs isolated from the placenta of healthy donors. The mean linear intercept (MLI) and mean alveolar number (MAN) were used to assess the degree of lung emphysema. IL-8 was measured using a radioimmunoassay, surfactant protein D (SP-D) was measured by ELISA, and matrix metalloproteinase (MMP)2 and MMP8 expression was assessed by PCR. Smoke fumigation combined to LPS injection successfully established a COPD rat model with significant emphysema and airway inflammation, elevated MLI and MAN, elevated systemic and lung tissue levels of IL-8 and SP-D ($P < 0.05$), and high expression of MMP2 and MMP8. Rats in the COPD + hAEC group exhibited alleviated lung damage, MLI and MAN ($P < 0.05$), reduced systemic and lung tissue levels of IL-8 and SP-D ($P < 0.05$) and MMP2 and MMP8 expression ($P < 0.05$). Early intervention using hAECs could delay disease progression in rats with COPD.

© 2016 The Authors. Published by Elsevier GmbH. This is an open access article under the CC BY license (http://creativecommons.org/licenses/by/4.0/).

1. Introduction

Chronic obstructive pulmonary disease (COPD) affects 329 million people worldwide [1]. COPD is characterized by the development of abnormal inflammatory responses to the inhalation of noxious particles, most commonly caused by long-term exposure to cigarette smoke. The pathological features of COPD include peripheral airway inflammation, lung parenchyma destruction, and emphysema [2]. Smoking can induce the aggregation and activation of alveolar macrophages and neutrophils, and trigger the release of elastase, especially matrix metalloproteinases (MMP), leading to emphysema and alveolar wall damage [3–5].

MMPs are mainly produced by neutrophils, alveolar macrophages, and airway epithelial cells. MMPs participate in airway inflammation by impairing the support of airway structural tissues, and by inducing chemotaxis, migration, and aggregation of inflammatory cells, as well as the release of various inflammatory cytokines and growth factors [6]. The neutrophil MMP2 and MMP8 belong to the gelatinase and collagenase subgroups, respectively, and can also induce the expression of IL-8, thereby further aggravating airway inflammation [7,8]. IL-8 is an important mediator of various inflammatory diseases, and mediates inflammatory reactions and immune regulation by regulating the aggregation and activation of neutrophils and T lymphocytes during inflammation [9,10]. IL-8 is recognized as a key factor to the development of COPD [9].

Studies have suggested that human amniotic epithelial cells (hAECs) can alleviate inflammation and play a role in the repair of lung injury by regulating the function of macrophages and reducing the aggregation of inflammatory cells [11–15]. The objective of this study was to investigate the effects of an early intervention using hAEC in a rat model of COPD. We established a rat model of COPD by LPS injection combined with cigarette smoke fumigation. During model establishment, rats in the COPD + hAEC group received intratracheal hAECs instillation. Results showed that hAECs infu-

* Corresponding author at: Graduate School, Hebei Medical University, Shijiazhuang 050017, China.
E-mail address: czq0423rsp@126.com (Z. Chen).

http://dx.doi.org/10.1016/j.prp.2016.08.014
0344-0338/© 2016 The Authors. Published by Elsevier GmbH. This is an open access article under the CC BY license (http://creativecommons.org/licenses/by/4.0/).

sion inhibited local and systemic inflammatory reactions that were exacerbated by COPD, thereby delaying the progress of COPD.

2. Materials and methods

2.1. Experimental animals

Twenty-four specific pathogen-free Wistar rats (male, weighing 240–260 g) were purchased from the Laboratory Animal Center of Hebei Medical University (production license number: SCXK (Hebei) 2008-1-003). All experiments were carried out in compliance with the NIH Guide for the Care and Use of Laboratory Animals (NIH Publication No. 85-23, revised 1996).

2.2. Animal grouping and treatment

Supplementary Fig. S1 in the online version at DOI: 10.1016/j.prp.2016.08.014 presents the study design. After a week of adaptive feeding (standard rat chow and free access to water), the 24 rats were randomized to three groups (n = 8/group): control, COPD, and COPD + hAEC groups. COPD was established in the COPD and COPD + hAEC groups by cigarette fumigation combined to lipopolysaccharides (LPS) injection. The hAEC intervention was administered to the COPD + hAEC group.

2.3. COPD model

Cigarette fumigation combined to LPS injection was performed as previously described [16]. On days 1 and 14 of model establishment, rats in the model group were administered 200 μL of 1 g/L LPS (Sigma L2880; 10 mg, USA) by tracheal injection, while the control rats were injected with 200 μL saline.

On days 2–13 d and 15–30 d of model establishment, the 24 rats were placed in a fumigating chamber (constructed by our laboratory). For each fumigating session, rats were exposed to the smoke of 15 cigarettes (Shijiazhuang cigarette factory, Shijiazhuang, China) for 20 min, twice daily, at an interval of 4 h. The fumigating chamber had three floors and rats were placed in the upper two floors. Ventilation openings were made at the top and bottom of the chamber, and the smoke-guiding tube directly conducted the smoke into the upper floors through the sidewalls of the chamber. The volume of the chamber was 160 L, and each cigarette produced approximately 500 mL of smoke, equivalent to a smoke concentration of approximately 5% for each fumigation. The control group was not given fumigation.

2.4. Preparation of human amniotic epithelial cells

hAECs were prepared as previously described [11,17]. Fresh human placenta was sampled from healthy women at term pregnancy (serum was tested to exclude any disease), and the amniotic membrane was mechanically separated and washed with PBS containing 50 μg/ml of gentamicin, 1.25 μg/ml of amphotericin B, 100 μg/ml of streptomycin, and 100 U/ml of penicillin (PBSA/GASP). The placenta was then cut into pieces of 2 × 2 mm and submerged in 0.02% EDTA-containing 0.05% trypsin (Sigma, St Louis, MO, USA) at 37 °C for 10 min. The digestion products were centrifuged for 30 min at 37 °C at 200 rpm. Single-cell suspension was obtained after filtering the product through a 250-mesh stainless steel sieve, and digestion was terminated by addition of medium containing 10% FBS. The cell suspension was then filtered through a 300-mesh stainless steel sieve, and the filtrate was centrifuged at 1500 rpm for 10 min. The supernatant was discarded and the cells were re-suspended. The suspension was then centrifuged at 800 rpm for 6 min and the supernatant was discarded, leaving hAECs at the bottom of the tube. Under light microscopy, the shape epithelial cells were oval and triangular; nuclei were obvious and the cytoplasm was homogeneous. The mouse anti-human cytokeratin 19 (CK19) immunohistochemistry kit (Maixin Biotech company) was used for immunohistochemistry. The epithelial cells were positive for this marker. After enzyme digestion, trypan blue staining was used for determining the proportion of living cells.

Cell counting using trypan blue staining showed that >90% of the cells were alive. hAECs were placed in the cell culture dishes at a density of 1×10^9 cells/L and incubated at 37 °C in a 5% CO_2 incubator. Cells were prepared for CK19 immunohistochemistry after the first passage. Cell growth was observed daily. Within 24 h after primary culture inoculation, adherent cell growth could be seen. After 72 h, cells showed rapid growth. Cells proliferated rapidly after each passage, and cell confluence reached >90%. Cells grew in the cobblestone-like shape, and were tightly packed. Cells were like flat irregular polygons, with clear outline, and abundant cytoplasm. A single cell was round or oval.

2.5. Flow cytometry

2.6. Intratracheal instillation of hAECs

On the first day of model establishment, rats in the COPD + hAECs group were anesthetized after LPS injection with 10% pentobarbital sodium (45 mg/kg, Sunshine Biotechnology Ltd., Shanghai, China) and given an intratracheal instillation of hAECs at a volume of 0.2 mL (containing 500,000 hAECs), as previously described [11,12].

2.7. Histological analysis

After model establishment (day 31), eight rats from each group were randomly selected and 5 mL of blood was sampled from their femoral artery. The right lower lung lobe was sampled and fixed in 10% formalin (Shanghai chemical Reagent Company, Shanghai, China) for 24 h. H&E staining and Masson's trichrome staining were performed using standard procedures. Pulmonary tissue morphology was observed under a DP73 digital microscope (Olympus, Tokyo, Japan) after paraffin embedding, sectioning, and H&E staining. The mean linear intercept (MLI) and mean alveolar number (MAN) were determined to assess the degree of lung emphysema. H&E-stained slides were photographed using a digital microscope, and the number of linings (NS) and the total alveolar count (Na) were measured to calculate the area of the image (S). The MLI and MAN was calculated according to the formula MLI = L/NS and MAN = Na/S. For each indicator, the average value calculated from eight randomly selected fields was used for statistical analysis.

Masson-trichrome staining was used for the assessment of collagen deposition using an AxioVision 3.1 image analysis system (Carl Zeiss GmbH, Oberkochen, Germany). Four to eight specimens of right lobe stained with Masson trichrome were selected. Digital images were taken at ×440 magnification. The area of collagen deposition (AC) and the perimeter of basement membrane of bronchioles (Pbm) beneath the basement membrane at 20 μm depth were measured as previously described [18]. Results are expressed as the area of collagen deposition (AC) per the perimeter of basement membrane of bronchioles (WAc/Pbm $\mu m^2/\mu m$). At least 10 bronchioles were counted on each slide.

2.8. Lung function

Lung function was assessed after measuring the weight gain of the rats, as previously described [19]. The rats were anesthetized by an intraperitoneal injection of 10% chloral hydrate (3 mL/kg). The rats were fixed on the operating table. The trachea was exposed and opened between the 2nd and 3rd cartilage rings, and rapidly intubated. After synchronization with the ventilator, lung function

was examined with a ML-V1-type pulmonary function analyzer for small laboratory animals and measurement software package (Beijing Yue Hongda LLC, Beijing, China). Resistance index (RI), forced expiratory volume (FEV), and forced vital capacity (FVC) were determined by the machine.

2.9. Determination of serum and tissue IL-8 content

Frozen serum samples (1 mL) and frozen lung tissue samples (50–100 mg) were used for IL-8 detection. The IL-8 levels of the serum and tissue homogenate (with 1 mL of cold PBS) were determined by radioimmunoassay (Purevalley Biotech, Beijing, China) according to the manufacturer's instructions using a FJ-2021 γ counter (Xian Nuclear Instrument Factory, Xian, China).

2.10. Bronchoalveolar lavage fluid

After completion of the lung function test, the animals were anesthetized with urethane (2 g/kg, i.p.). Bronchoalveolar lavage fluids (BALF) were obtained using a tracheal tube. The lungs were washed thrice with 0.5 mL of sterilized normal saline containing 1% bovine serum albumin (BSA) and 5000 IU/l heparin. BALF was diluted with 1.5 mL of Hank's balanced salt solution (HBSS) containing 2% fetal calf serum. The samples were centrifuged at 500*g* at 4 °C for 10 min. The pellets were resuspended with HBSS. The samples were stained with the Wright-Giemsa staining and 200 cells were classified under light microscopy. The results were expressed as the numbers of cells of each type of cell population in one liter of BALF, as previously described [20].

2.11. Serum and tissue SP-D content

The surfactant protein D (SP-D) levels of the serum and tissue samples were measured by ELISA (Westang Ltd. Co., Shanghai, China), according to the manufacturers' instructions.

2.12. MMP2 and MMP8 expression in lung tissue

The levels of MMP2 and MMP8 expression in lung tissue were assessed by PCR using the primers listed in Table 1, a PE9600 PCR thermocycler, and total RNA extraction kit, DNase, cDNA synthesis kit, PCR reaction system, agarose, and Spain DNA Marker (Takara Bio, Otsu, Japan).

Standard gel zymography was used to measure levels of MMP-2 and MMP-8. The proteins were extracted from lung tissue and total protein concentrations were determined with the BCA assay (Pierce Chemical, Dallas, TX, USA). Thirty micrograms of total protein were loaded and separated by a 10% Tris-glycine gel with 0.1% gelatin as substrate, washed with renaturing buffer (Invitrogen Inc., Carlsbad, CA, USA) for 90 min and further incubated with developing buffer (Invitrogen Inc., Carlsbad, CA, USA) at 37 °C for 24 h. Finally, the gels were stained with 0.5% Coomassie blue R-250 for 1 h and then destained appropriately. MMP-2 and MMP-8 human standards (same molecular weight as the rat proteins) were loaded in each gel to identify the bands and to standardize the measurements among gels. Band intensities of total MMP-8 and MMP-2 (including pro- and cleaved forms) were quantified using standard gel densitometry techniques.

2.13. Total MMP activity assay

The total activity of MMPs was determined using a GenMed MMP Fluorimetric Assay Kit (GenMed Scientifics Inc., Shanghai, China), according to the manufacturer's instructions. Briefly, the proteins were extracted from lung tissue and total protein concentrations were determined with the BCA assay (Pierce Chemical, Dallas, TX, USA). Protein samples (50 μL) were added to a reaction mixture containing the MMP fluorescence resonance energy transfer peptide substrate, Mca-PLGL-Dap-(Dnp)-AR-OH [21]. After 40 min of incubation at 37 °C, the fluorescence intensity was measured at 330 nm/400 nm (excitation/emission) with a fluorescence microplate reader, using 7-methoxycourmarin (MCA) as the standard. One unit of MMP activity was defined as the amount of enzyme hydrolyzing 1 nmol of peptide substrate per min at 37 °C at pH 7.5.

2.14. Statistical analysis

Statistical analysis was performed using SPSS 13.0 software. Data normality was tested by the Kolmogorov-Smirnov test, and homogeneity of variance was tested using one-way ANOVA. Measurement data with normal distribution were presented as mean ± standard deviation, and measurement data without normal distribution were presented as medians and interquartile ranges. Indicators with normal distribution and homogeneity of variance were analyzed with one-way ANOVA modeled for a completely randomized design with the SNK-q post hoc test. Indicators without homogeneity of variance were analyzed by the nonparametric Kruskal-Wallis H test for independent samples, and inter-group comparisons were made by the Mann-Whitney *U* test. Statistical significance was defined at $P < 0.05$.

3. Results

3.1. Establishment of a rat model of COPD and hAEC intervention

One month after establishment of the model, the weight of COPD rats was lower than that of the control rats ($P < 0.05$), while the weight of the COPD + hAEC rats was higher than that of the COPD rats (Table 2).

Rats in the COPD + hAEC group received intra-tracheal instillation of 500,000 hAECs on the first day of COPD model establishment, after injection of LPS, as previously described [11,12,22]. Rats that received early intervention exhibited an intermediate status with slight coughing and irritability, but had no sputum or wheezing.

3.2. Lung function

Lung function tests showed that the model group had a higher RI than controls ($P < 0.05$) and lower FEV0.3 and FEV0.3/FVC (both $P < 0.05$). The COPD + hAEC group showed lung functions that were intermediary to the control and model groups, but nevertheless significantly lower than in the model group ($P < 0.05$) (Table 2).

3.3. Pulmonary histopathology

The lungs of the control rats showed no significant inflammatory cell infiltration and no thickening of the bronchial mucosa, but a neat arrangement of bronchial epithelial cilia with no loss, thinning, or rupturing of the alveolar walls, and no bullous formation (Fig. 1). In contrast, the lungs of COPD rats exhibited chronic inflammatory cell infiltration (mainly macrophages, lymphocytes, and monocytes), bronchial mucosal thickening, cilia loss, mucous plug formation, and chronic inflammatory cell infiltration at airway, alveolar wall rapture, and bullous formation, as well as thickening of the vessel walls. The COPD model rats exhibited centrilobular emphysema (Fig. 1A). Rats that received hAEC intervention also exhibited the pathological changes observed in COPD rats, but the level of inflammatory cell infiltration was lower, and tissue damage caused by lobular emphysema was alleviated (Fig. 1B).

The MLI of COPD rats ($13.3 \pm 1.6 \times 10^{-5}$/m) was significantly higher than in control rats ($8.3 \pm 0.6 \times 10^{-5}$/m), while MAN of COPD

Table 1
PCR primers.

Gene	Primers	Product (base pairs)	Annealing temperature (°SC)
MMP2	F 5′-ACGATGATGACCGGAAGTGG-3′ R 5′-GTGCTGGCAGAATAGACCCA-3′	505	53
MMP8	F 5′-TCCAGGTTACCCCACTAGCA-3′ R 5′-TGCAACTCTAGTGACTCTGCG-3′	151	52
GAPDH	F 5′-GCAACTCCCATTCTTCCACC-3′ R 5′-TGGTATTCGAGAGAAGGGAGGG-3′	322	54

Table 2
Comparison of weight and lung function tests in the three groups.

	Weight	RI ($cmH_2O\ ml^{-1}\ s^{-1}$)	FEV0.3 (mL)	FEV0.3/FVC (%)
Control	366.4 ± 14.2	0.3 ± 0.1	5.0 ± 0.4	94.1 ± 3.3
COPD	301.8 ± 16.0*	0.7 ± 0.1*	3.8 ± 0.3*	63.8 ± 5.0*
COPD + hAEC	346.9 ± 10.7*,**	0.5 ± 0.1*,**	4.5 ± 0.4*, **	79.9 ± 4.6*, **

n = 8/group.
RI: resistance index; FEV: forced expiratory volume; FVC: forced vital capacity.
* P < 0.05 vs. the control group.
** P < 0.05 vs. the COPD group.

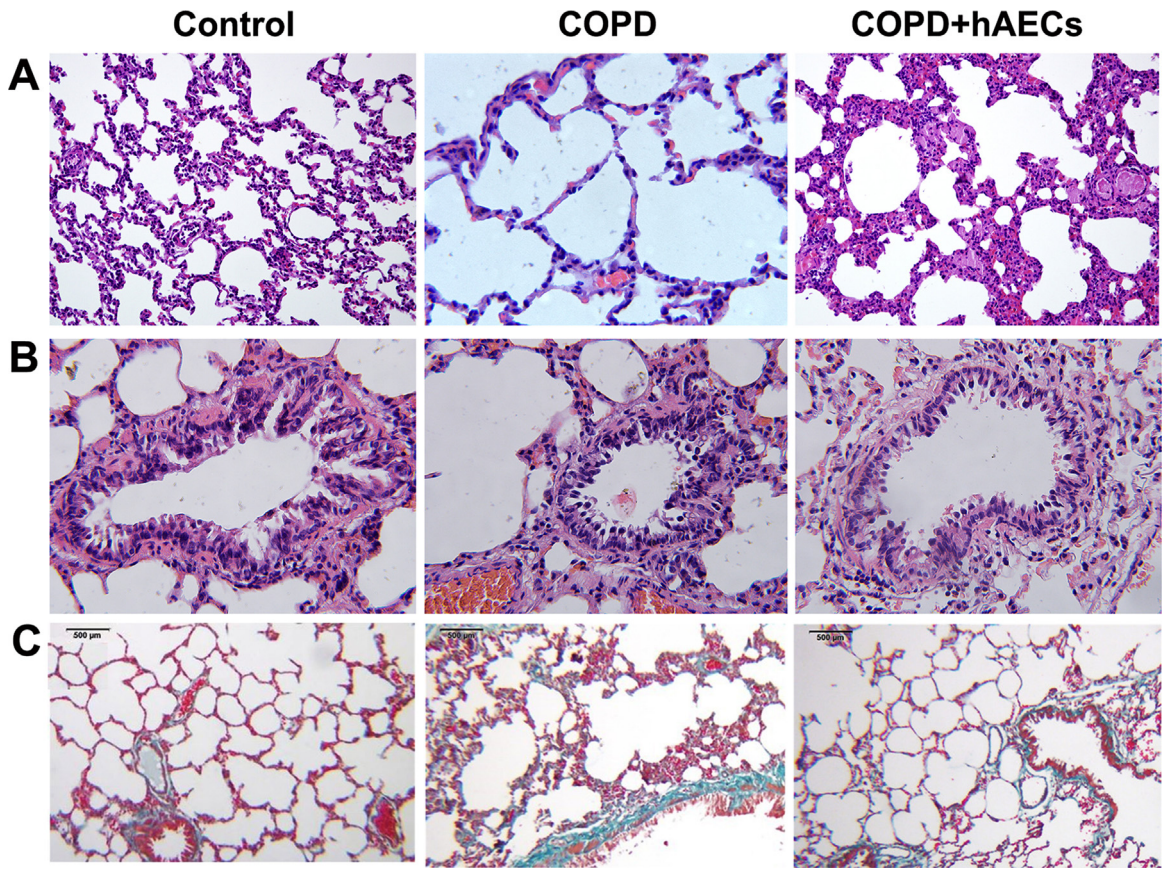

Fig. 1. Pulmonary histopathology. (A) H&E staining of lung tissues of rats in the control, COPD, and COPD + hAEC groups (×200). (B) H&E staining of lung tissues showing inflammatory cell infiltration. (C) Masson staining of lung tissues of rats in the control, COPD, and COPD + hAEC groups. Bar = 500 μm.

Table 3
Histological characteristics of the three groups.

Group	MLI ($\times 10^{-5}$m)	MAN ($\times 10^7/m^2$)
Control	8.3 ± 0.6	11.4 ± 2.3
COPD	13.3 ± 1.6*	5.0 ± 0.9*
COPD + hAEC	11.2 ± 0.8*,**	6.8 ± 1.2*, **

n = 8/group.
MLI: mean linear intercept; MAN: mean alveoli number.
* P < 0.05 vs. the control group.
** P < 0.05 vs. the COPD group.

Table 4
Effect of hAECs on collagen deposition in lungs.

	Collagen deposition (WAc/Pbm, $\mu m^2/\mu m$)
Control	2.6 ± 0.6
COPD	$6.9 \pm 0.9^{*}$
COPD + hAEC	$4.6 \pm 0.8^{*,**}$

n = 8/group.
* P < 0.05 vs. the control group.
** P < 0.05 vs. the COPD group.

rats ($5.0 \pm 0.8 \times 10^7/m^2$) was significantly lower than in control rats ($11.4 \pm 2.3 \times 10^7/m^2$). Both indexes were significantly better in COPD + hAEC rats ($11.2 \pm 0.8 \times 10^{-5}/m$ and $6.8 \pm 1.2 \times 10^7/m^2$) ($P < 0.05$) (Table 3).

The COPD group showed more collagen deposition than the control group (P < 0.05). The COPD + hAEC group showed an amount of collagen deposition intermediary between the control and COPD groups, but lower than that of the COPD group (P < 0.05) (Fig. 1C and Table 4).

3.4. Lung inflammation

The white blood cell counts and neutrophils proportions in BALF of the COPD group were higher than that of the control and COPD + hAECs groups, while macrophage and lymphocyte proportions in the BALF of the COPD group were lower than that of the control and COPD + hAECs groups (Table 5).

3.5. Pulmonary and systemic IL-8 and SP-D levels

The serum and tissue levels of IL-8 in COPD rats (0.47 ± 0.10 ng/ml and 0.40 ± 0.37 ng/ml) was significantly higher than that of control rats (0.24 ± 0.09 ng/ml and 0.24 ± 0.04 ng/ml) ($P < 0.05$), but both measurements were significantly improved by hAEC intervention (0.32 ± 0.10 ng/ml and 0.24 ± 0.02 ng/ml) ($P < 0.05$), reducing the levels of IL-8 in the serum and tissue to the baseline levels observed in control animals (P > 0.05) (Table 6).

The serum and tissue levels of SP-D in COPD rats (55.99 ± 7.81 ng/ml and 37.63 ± 7.70 ng/ml) was significantly higher than in control rats (28.44 ± 4.26 ng/ml and 68.23 ± 6.55 ng/ml) ($P < 0.05$), but both measurements were significantly improved by hAEC intervention (37.62 ± 6.55 ng/ml and 44.13 ± 10.29 ng/ml) ($P < 0.05$), reducing the levels of SP-D in the serum and tissue to the baseline levels observed in control animals (P > 0.05) (Table 6).

3.6. Pulmonary and systemic MMP2 and MMP8 expression

RT-PCR was performed to detect MMP2 and MMP8 mRNA expression in lung tissues of rats. MMP2 and MMP8 expression was significantly higher in COPD rats compared with controls, but significantly decreased in COPD + hAECs rats compared with COPD rats (Fig. 2).

Table 6
IL-8 and pulmonary SP-D levels among groups.

	Group	IL-8 (ng/ml)	SP-D (ng/ml)
Serum	Control	0.24 ± 0.09	28.44 ± 4.26
	COPD	$0.47 \pm 0.10^{*}$	$55.99 \pm 7.81^{*}$
	COPD + hAEC	$0.32 \pm 0.10^{**,\#}$	$37.62 \pm 6.55^{*,\#}$
Tissue	Control	0.24 ± 0.04	37.63 ± 7.70
	COPD	$0.40 \pm 0.37^{*}$	$68.23 \pm 6.55^{*}$
	COPD + hAEC	$0.24 \pm 0.02^{*,**}$	$44.13 \pm 10.29^{*,\#}$

n = 8/group.
SP-D: surfactant protein D.
* P < 0.05 vs. the control group.
** P > 0.05 vs. the control group.
# P < 0.05 vs. the COPD group.

Table 7
Comparison of MMP8 and MMP2 activity among groups.

	MMP2 (U/mg of protein)	MMP8 (U/mg of protein)
Control	3.00 ± 0.62	0.42 ± 0.04
COPD	$4.86 \pm 0.36^{*}$	$0.60 \pm 0.05^{*}$
COPD + hAEC	$3.990.50^{*,**}$	$0.53 \pm 0.03^{*,**}$

n = 8/group.
* P < 0.05 vs. the control group.
** P < 0.05 vs. the COPD group.

3.7. MMP2 AND MMP8 activity

MMP2 and MMP8 activity was higher in the COPD group compared with the control group (P < 0.05), while the COPD + hAEC group showed MMP2 and MMP8 activity that was intermediary to that of the control and COPD groups, but lower than that of the COPD group) P < 0.05) (Table 7).

4. Discussion

hAECs have been reported to regulate inflammatory reactions and mediate lung injury repair [11–15]. This study aimed to investigate the effects of hAEC early intervention in a rat model of COPD. We established a rat model of COPD by LPS injection combined with smoke fumigation. During model establishment, rats in the AEC group received intratracheal hAEC instillation.

Smoke fumigation combined to LPS injection was used successfully to establish a rat model of COPD with significant emphysema and airway inflammation, elevated MLI and MAN, and elevated systemic and lung tissue levels of IL-8. IL-8 is recognized as a key factor of the development of COPD [9]. COPD model animals also exhibited elevated SP-D levels, and enhanced expression of MMP2 and 8. Previous reports have highlighted the elevation of serum and bronchoalveolar lavage SP-D levels in patients with COPD, and that SP-D levels were positively associated with patients' history and amount of cigarette smoking [3–5]. MMPs have been implicated in the induction of emphysema and alveolar wall damage [3–5].

Increased serum levels of SP-D indicate damage of pulmonary tissues and decline of lung function, while decreased SP-D in the serum and increased SP-D in bronchoalveolar lavage fluid indicate alleviation of COPD, which is of great significance for disease

Table 5
White blood cell count and classification in BALF.

	WBC ($\times 10^5$ cells/ml)	Neutrophils (%)	Macrophages (%)	Lymphocytes (%)
Control	4.0 ± 0.8	2.3 ± 1.0	87.2 ± 5.7	10.2 ± 3.2
COPD	$9.8 \pm 1.1^{*}$	$24.5 \pm 6.1^{*}$	$69.1 \pm 7.6^{*}$	$6.4 \pm 2.3^{*}$
COPD + hAEC	$6.2 \pm 1.0^{*,**}$	$6.1 \pm 2.7^{*,**}$	$79.7 \pm 6.7^{*,**}$	$14.2 \pm 4.3^{*,**}$

n = 8/group.
* P < 0.05 vs. the control group.
** P < 0.05 vs. the COPD group.

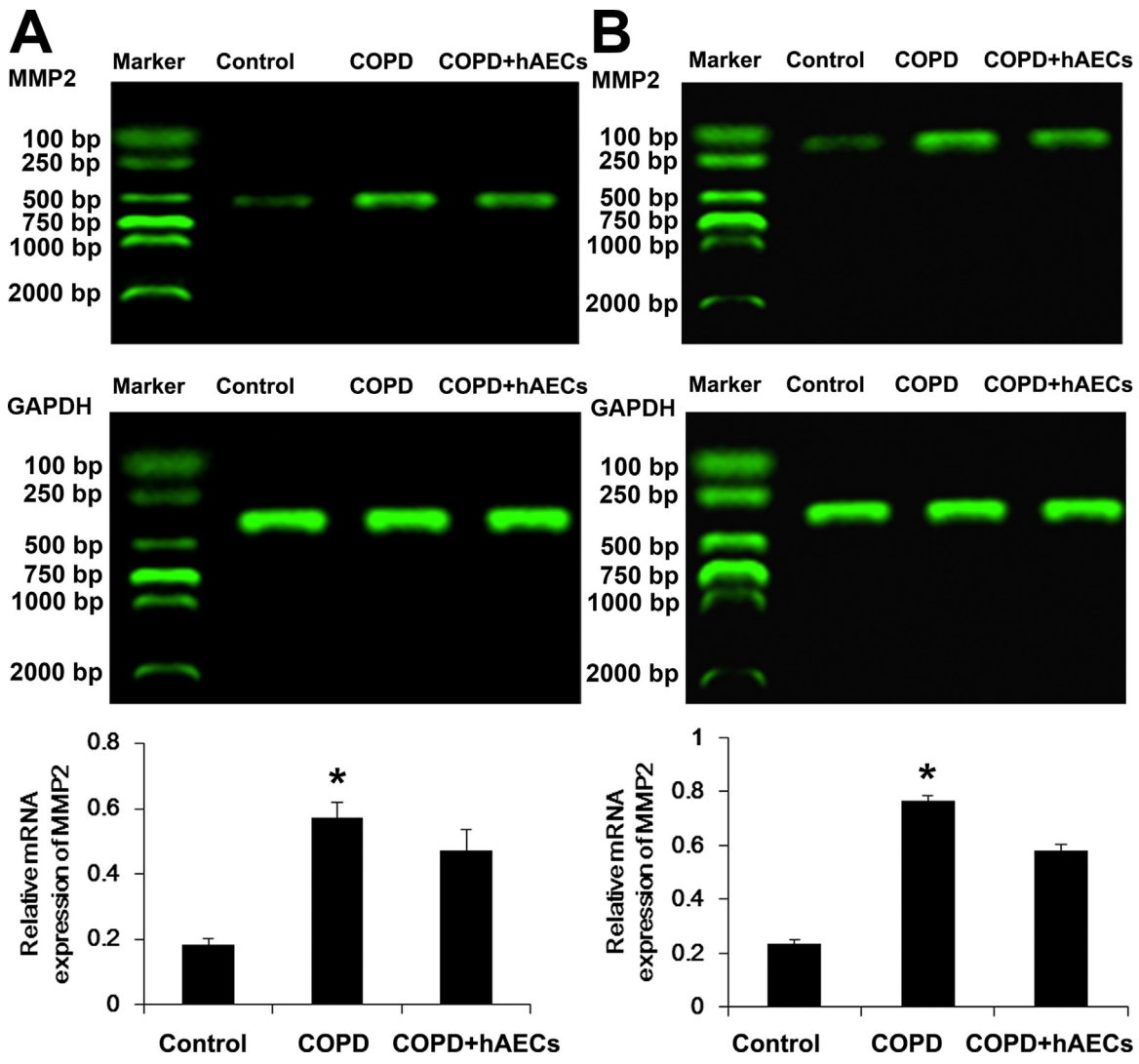

Fig. 2. MMP2 and MMP8 expression in lung tissues. A, mRNA expression of MMP2; B, mRNA expression of MMP8. *P < 0.05 compared with Con group.

monitoring and prognosis [23]. SP-D could be an indicator for inflammation monitoring and prognosis during COPD and its treatments.

Developing a drug or biological agent that could reduce inflammation should help delaying the progress of COPD. In the present study, hAEC infusion inhibited local and systemic inflammatory reactions that were exacerbated by COPD, thereby delaying the progress of COPD. Rats in the COPD + hAEC group exhibited alleviated lung damage, MLI and MAN, reduced systemic and lung tissue levels of IL-8 and SP-D, and MMP2 and MMP8 expression. These indexes not only indicate that hAEC infusion effectively reduced inflammation, but that this process could be measured in the circulating blood, allowing the therapeutic intervention to be easily monitored.

The human amnion is the tissue located at the innermost layer of the human placenta, and as is widely available and easily collected. hAECs may retain some or even full multi-differentiation potential, exhibiting a higher degree of stem-ability, and high similarity to embryonic stem cells [7]. Due to their anti-inflammatory and regenerative features, hAECs may represent a promising cellular treatment for COPD, and these therapies should be further investigated in a wider range of animal models of inflammatory diseases [24].

Of course, the present study is not without limitations. All models of chronic lung injury have their strengths and limitations [25]. In addition, it has to be highlighted that the present study used hAECs as prevention and not as treatent of COPD, as previously suggested [26]. Finally, the effects of hAECs on rate without CPOD were not investigated. Additional studies are necessary to examine the effects of hAECs on chronic inflammatory lung diseases.

In this study, hAECs instillation was conducted during the first stage of COPD model establishment. This reduced the damage to MLI, decreased serum and tissue IL-8 and SP-D levels, improved alveolar surface area, and prevented bullae formationDelayed COPD progression after early intervention might be attributed to the anti-inflammatory role of hAECs. However, whether this result could be achieved with intraperitoneal injection or intravenous injection, and whether this is associated with the regenerative capability of hAECs requires further investigation.

References

[1] The 10 leading causes of death in the world, 2000 and 2011. World Health Organization. July 2013. http://who.int/mediacentre/factsheets/fs310/en/ Retrieved November 29, 2013.

[2] N. Tanabe, Y. Hoshino, S. Marumo, H. Kiyokawa, S. Sato, D. Kinose, K. Uno, S. Muro, T. Hirai, J. Yodoi, M. Mishima, Thioredoxin-1 protects against neutrophilic inflammation and emphysema progression in a mouse model of

chronic obstructive pulmonary disease exacerbation, PLoS One 8 (2013) e79016.
[3] Q. Wang, Y. Wang, Y. Zhang, Y. Zhang, W. Xiao, Involvement of urokinase in cigarette smoke extract-induced epithelial-mesenchymal transition in human small airway epithelial cells, Lab. Invest. 95 (2015) 469–479.
[4] J.L. Tan, S.T. Chan, E.M. Wallace, R. Lim, Human amnion epithelial cells mediate lung repair by directly modulating macrophage recruitment and polarization, Cell Transplant. 23 (2014) 319–328.
[5] C. Donovan, H.J. Seow, S.G. Royce, J.E. Bourke, R. Vlahos, Alteration of airway reactivity and reduction of ryanodine receptor expression by cigarette smoke in mice, Am. J. Respir. Cell Mol. Biol. 53 (2015) 471–478.
[6] D.E. Davies, J. Wicks, R.M. Powell, S.M. Puddicombe, S.T. Holgate, Airway remodeling in asthma: new insights, J. Allergy Clin. Immunol. 111 (2003) 215–225, quiz 26.
[7] A. Toda, M. Okabe, T. Yoshida, T. Nikaido, The potential of amniotic membrane/amnion-derived cells for regeneration of various tissues, J. Pharmacol. Sci. 105 (2007) 215–228.
[8] G.A. Finlay, L.R. O'Driscoll, K.J. Russell, E.M. D'Arcy, J.B. Masterson, M.X. FitzGerald, C.M. O'Connor, Matrix metalloproteinase expression and production by alveolar macrophages in emphysema, Am. J. Respir. Crit. Care Med. 156 (1997) 240–247.
[9] X. Zhang, H. Zheng, H. Zhang, W. Ma, F. Wang, C. Liu, S. He, Increased interleukin (IL)-8 and decreased IL-17 production in chronic obstructive pulmonary disease (COPD) provoked by cigarette smoke, Cytokine 56 (2011) 717–725.
[10] G. Deslee, S. Dury, J.M. Perotin, D. Al Alam, F. Vitry, R. Boxio, S.C. Gangloff, M. Guenounou, F. Lebargy, A. Belaaouaj, Bronchial epithelial spheroids: an alternative culture model to investigate epithelium inflammation-mediated COPD, Respir. Res. 8 (2007) 86.
[11] P. Vosdoganes, R.J. Hodges, R. Lim, A.J. Westover, R.Y. Acharya, E.M. Wallace, T.J. Moss, Human amnion epithelial cells as a treatment for inflammation-induced fetal lung injury in sheep, Am. J. Obstet. Gynecol. 205 (2011) e26–e33, 156.
[12] P. Vosdoganes, R. Lim, E. Koulaeva, S.T. Chan, R. Acharya, T.J. Moss, E.M. Wallace, Human amnion epithelial cells modulate hyperoxia-induced neonatal lung injury in mice, Cytotherapy 15 (2013) 1021–1029.
[13] A. Cargnoni, M. Di Marcello, M. Campagnol, C. Nassuato, A. Albertini, O. Parolini, Amniotic membrane patching promotes ischemic rat heart repair, Cell Transplant. 18 (2009) 1147–1159.
[14] Y. Moodley, S. Ilancheran, C. Samuel, V. Vaghjiani, D. Atienza, E.D. Williams, G. Jenkin, E. Wallace, A. Trounson, U. Manuelpillai, Human amnion epithelial cell transplantation abrogates lung fibrosis and augments repair, Am. J. Respir. Crit. Care Med. 182 (2010) 643–651.
[15] S.V. Murphy, S.C. Shiyun, J.L. Tan, S. Chan, G. Jenkin, E.M. Wallace, R. Lim, Human amnion epithelial cells do not abrogate pulmonary fibrosis in mice with impaired macrophage function, Cell Transplant. 21 (2012) 1477–1492.
[16] Y.C. Nie, H. Wu, P.B. Li, Y.L. Luo, C.C. Zhang, J.G. Shen, W.W. Su, Characteristic comparison of three rat models induced by cigarette smoke or combined with LPS: to establish a suitable model for study of airway mucus hypersecretion in chronic obstructive pulmonary disease, Pulm. Pharmacol. Ther. 25 (2012) 349–356.
[17] S. Murphy, S. Rosli, R. Acharya, L. Mathias, R. Lim, E. Wallace, G. Jenkin, Amnion epithelial cell isolation and characterization for clinical use, Curr. Protoc. Stem Cell Biol. (2010), Chapter 1 Unit 1E 6.
[18] E. Palmans, J.C. Kips, R.A. Pauwels, Prolonged allergen exposure induces structural airway changes in sensitized rats, Am. J. Respir. Crit. Care Med. 161 (2000) 627–635.
[19] Y. Wang, X. Jiang, L. Zhang, L. Wang, Z. Li, W. Sun, Simvastatin mitigates functional and structural impairment of lung and right ventricle in a rat model of cigarette smoke-induced COPD, Int. J. Clin. Exp. Pathol. 7 (2014) 8553–8562.
[20] Z.S. Bao, L. Hong, Y. Guan, X.W. Dong, H.S. Zheng, G.L. Tan, Q.M. Xie, Inhibition of airway inflammation, hyperresponsiveness and remodeling by soy isoflavone in a murine model of allergic asthma, Int. Immunopharmacol. 11 (2011) 899–906.
[21] J.L. Lauer-Fields, T. Broder, T. Sritharan, L. Chung, H. Nagase, G.B. Fields, Kinetic analysis of matrix metalloproteinase activity using fluorogenic triple-helical substrates, Biochemistry 40 (2001) 5795–5803.
[22] T. Liu, J. Wu, Q. Huang, Y. Hou, Z. Jiang, S. Zang, L. Guo, Human amniotic epithelial cells ameliorate behavioral dysfunction and reduce infarct size in the rat middle cerebral artery occlusion model, Shock 29 (2008) 603–611.
[23] C.R. Ju, W. Liu, R.C. Chen, Serum surfactant protein D: biomarker of chronic obstructive pulmonary disease, Dis. Mark. 32 (2012) 281–287.
[24] T. Miki, S.C. Strom, Amnion-derived pluripotent/multipotent stem cells, Stem Cell Rev. 2 (2006) 133–142.
[25] J.L. Wright, M. Cosio, A. Churg, Animal models of chronic obstructive pulmonary disease, Am. J. Physiol. Lung Cell. Mol. Physiol. 295 (2008) L1–L15.
[26] A. Churg, D.D. Sin, J.L. Wright, Everything prevents emphysema: are animal models of cigarette smoke-induced chronic obstructive pulmonary disease any use? Am. J. Respir. Cell Mol. Biol. 45 (2011) 1111–1115.